Journal of Alloys and Compounds 526 (2012) 135–138

Contents lists available at SciVerse ScienceDirect

Journal of Alloys and Compounds

journal homepage: www.elsevier.com/locate/jallcom

Codoping effect of $Li_{1.1}V_{0.9}O_2$ anodes for lithium-ion batteries with Mo and W ($Li_{1.1}V_{0.9-2x}Mo_xW_xO_2$): Based on electronic structure calculations using full-potential KKR-Green's function method

Hyung Sun Kim [a], Hannah Song [b], Ji Kwon Jung [a], Byung-Ki Na [c], Byung Won Cho [a], Yong-Tae Kim [b,*]

[a] Center for Energy Convergence, Korea Institute of Science and Technology (KIST), P.O. Box 131, Cheongryang, Seoul 130-650, Republic of Korea
[b] Energy System Major, School of Mechanical Engineering, Pusan National University, Busan 609-735, Republic of Korea
[c] Department of Chemical Engineering, Chungbuk National University, Chungbuk 361-763, Republic of Korea

ARTICLE INFO

Article history:
Received 27 August 2011
Accepted 10 February 2012
Available online xxx

Keywords:
Lithium vanadium oxide
Anode
Density of state
Lithium batteries

ABSTRACT

Pure crystalline doped $Li_{1.1}V_{0.9}O_2$ powder was prepared. The specific charge/discharge capacities of the doped $Li_{1.1}V_{0.9}O_2$ anodes were more than double of those of the bare $Li_{1.1}V_{0.9}O_2$ anodes, especially at high *C*-rates. The main origin of such capacities was revealed to be the increase in electronic conductivity upon doping due to the extra free electron.

1. Introduction

New alternative anode materials have been investigated for use in lithium-ion batteries to meet the requirements for portable power sources with high specific capacities [1–3]. Of these, lithium vanadate materials have been proposed as anode materials to replace lithium metal and carbonaceous materials. $Li_{1.1}V_{0.9}O_2$ has a high specific capacity of 1200 mAh/cc on a volume basis, and a low working potential below 0.3 V vs. Li/Li^+ [4–6], so further research on the structure and valence state of this material is desirable because of its potential application as an anode material [7,8].

However, without any material modifications, the electrochemical properties of such materials, in particular their rather low electronic conductivities, are still insufficient, particularly for high-current applications. A carbon coating has been considered as a possible solution, but there has been no report on doping with other metals to increase the electronic conductivity of $Li_{1.1}V_{0.9}O_2$ for the enhancement of its rate capability [9].

In this work, the effect of the codoping of Mo and W into a $Li_{1.1}V_{0.9}O_2$ ($Li_{1.1}V_{0.9-2x}W_xMo_xO_2$) anode was studied through electronic structure calculations. In particular, the projected density of states (PDOS) for each Mo and W was carefully investigated to understand the individual doping effects on the enhancement of the anode performance in lithium-ion batteries.

2. Experimental

The preparation of the $Li_{1.1}V_{0.9-2x}W_xMo_xO_2$ ($x = 0, 0.025, 0.075$) active materials was carried out by conventional solid-state reactions. Stoichiometric amounts of Li_2CO_3 (Aldrich, 99.8%), V_2O_3 (Alfa Aesar, 99.7%), WO_2 (Aldrich, 99.8%), and MoO_2 (Aldrich, 99.8%) precursors were milled in a planetary ball-milling machine (Pulverisette 7, Fritsch) at a rotation speed of 250 rpm for 1 h. Sintering was then performed in two steps: 500 °C for 6 h and 1100 °C for 10 h in an atmosphere of N_2 with 10 mol% H_2. The crystal structure of the powder was analyzed by X-ray diffraction (XRD, Rigaku D/MAX-2500 V).

The electrodes were prepared by mixing the obtained $Li_{1.1}V_{0.9-2x}W_xMo_xO_2$ active material (90 wt%), Denka Black (5 wt%), PVdF (5 wt%), and NMP solvent in a high-speed mixer. They were assembled with a lithium foil electrode using CR2032 coin cells in a dry room. A microporous polypropylene separator (Celgard 2400) was used. The electrolyte was 1 M $LiPF_6$ in a mixed solvent of ethylene carbonate (EC) and diethyl carbonate (DEC) (3:7 by volume). The cells were tested by galvanostatic measurements in the voltage range 0.01–2.0 V vs. Li/Li^+ using a Maccor system (S 4000, USA).

The electronic structure and projected density of states (PDOS) of $Li_{1.1}V_{0.9-2x}W_xMo_xO_2$ ($x = 0$, 0.025, 0.075) were calculated by using the FEFF 8.4 code based on the KKR-Green's function method [10]. The SCF, FMS, and EXCHANGE cards for full multi-scattering and self-energy calculations based on the Hedin–Lundqvist model were employed to calculate the Fermi energy and charge transfer.

3. Results and discussion

As seen in Fig. 1, the XRD patterns from the bare $Li_{1.1}V_{0.9}O_2$ and $Li_{1.1}V_{0.9-2x}Mo_xW_xO_2$ powders demonstrate that they have a

* Corresponding author. Tel.: +82 51 510 1012; fax: +82 51 514 0685.
E-mail address: yongtae@pusan.ac.kr (Y.-T. Kim).

0925-8388/$ – see front matter © 2012 Elsevier B.V. All rights reserved.
doi:10.1016/j.jallcom.2012.02.073

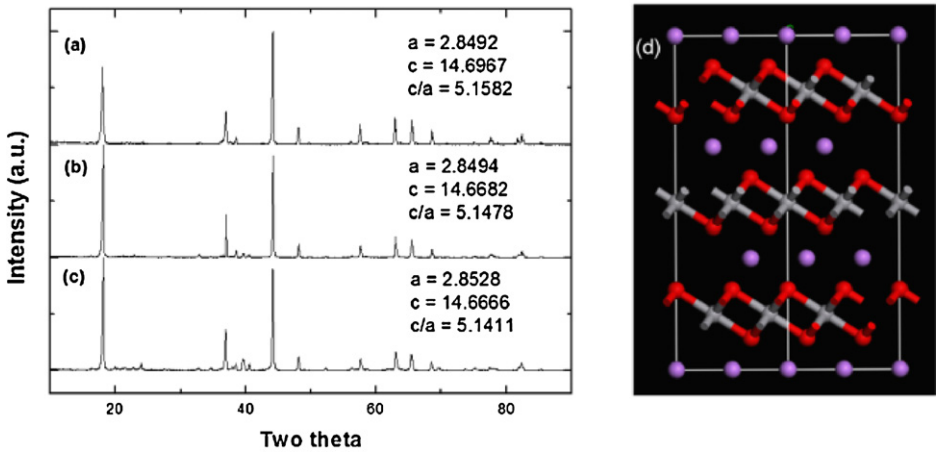

Fig. 1. XRD patterns of the synthesized $Li_{1.1}V_{0.9-2x}Mo_xW_xO_2$ powders: (a) $x = 0$, (b) $x = 0.025$, (c) $x = 0.075$,and (d) the lattice structure on the {1 1 0} plane of lithium vanadium oxide (Li, purple; V, grey; O, red). (For interpretation of the references to color in this figure legend, the reader is referred to the web version of the article.)

layered structure (space group *R*-3*m*). Fig. 1(d) shows the lattice structure on the {1 1 0} plane, in which V and O form a VO_6 octahedral structure. The lattice parameters of the synthesized $Li_{1.1}V_{0.9-2x}Mo_xW_xO_2$ powders are summarized in Fig. 1. The cell parameters *a* and *c* are changed slightly upon doping with Mo and W, and it is readily recognized that with the increase in the amount of doping with Mo and W, the lattice parameter of the *a*-axis increases, while that of the *c*-axis decreases. That is, the atomic bond lengths between atoms in the same layer increase, while the interactions between layers become stronger. In order to understand the origin of this structural change, an electronic structure analysis was carried out using the FEFF 8.4 code.

Fig. 2(a) and (b) shows the PDOS for $Li_{1.1}V_{0.9}O_2$ and $Li_{1.1}V_{0.8}Mo_{0.05}W_{0.05}O_2$, respectively. In the case of $Li_{1.1}V_{0.9}O_2$, the V 3d band is positioned across the Fermi level, which means that $Li_{1.1}V_{0.9}O_2$ is already an electronic conductor without any doping with transition metals. In particular, the strong overlapping of the DOS for the V 3d band and the O 2p band between about −10 and −5 eV indicates that there is a strong covalent bond between V and O [7]. Overall, similar results were obtained for $Li_{1.1}V_{0.8}W_{0.05}Mo_{0.05}O_2$ and $Li_{1.1}V_{0.9}O_2$, as shown in Fig. 2(b). It is interesting to note that there is a clear difference between Mo and W in the localized electronic structure (PDOS). The shape and bandwidth of the Mo 4d band is similar to the V 3d band, for which the PDOS is concentrated near the Fermi level, implying that there is a strong interaction between the Mo 4d and V 3d bands. On the other hand, the W 5d band is relatively broad, and thereby has a weaker interaction than the Mo 4d band with the V 3d band. Such a difference in electronic structure for Mo and W as dopants is attributable to their different atomic radii and electron arrangements ($4d^5 5s^1$ for Mo and $5d^4 6s^2$ for W). That is, in the case of W, since the principal quantum number and the proportion of s-character electrons is higher than for Mo, the band structure is much broader, and therefore the electronic interactions to form bonds with O and Li are clearly weaker.

Table 1 shows the electron densities for $Li_{1.1}V_{0.9}O_2$ and $Li_{1.1}V_{0.8}W_{0.05}Mo_{0.05}O_2$. First, it can be readily recognized that the electron density is increased overall after doping with Mo and W. While the electron densities of Li is reduced upon doping, those of V and O are increased. This is consistent with the results on the band structure (PDOS), which show a broader band for W (Fig. 2(b)), implying that there is little change in electron density because of the weaker electronic interaction for W. The extra electron from doping with the donors Mo and W, occupying the 3b octahedral site, is provided mainly to the V 3d and O 2p bands, so that their ionic radii increase. Hence, this is the main origin of the increase in the *a*-axis lattice parameter, as shown in Fig. 1. Even though the increased bond length between V and O due to the expanded ionic radius could also increase the *c*-axis lattice parameter, we should consider the Coulombic interactions between the layers as well as the atomic bond lengths in order to understand the changes in lattice structure in more detail. The Coulombic interactions between the V and O layers can be neglected, because there is little change

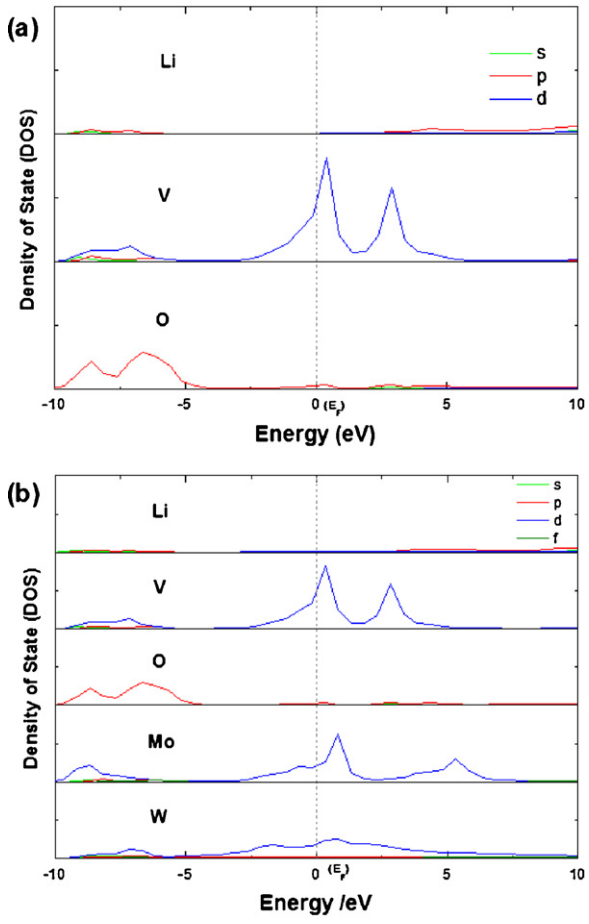

Fig. 2. Projected density of states (PDOS) of (a) $Li_{1.1}V_{0.9}O_2$ and (b) $Li_{1.1}V_{0.8}Mo_{0.05}W_{0.05}O_2$.

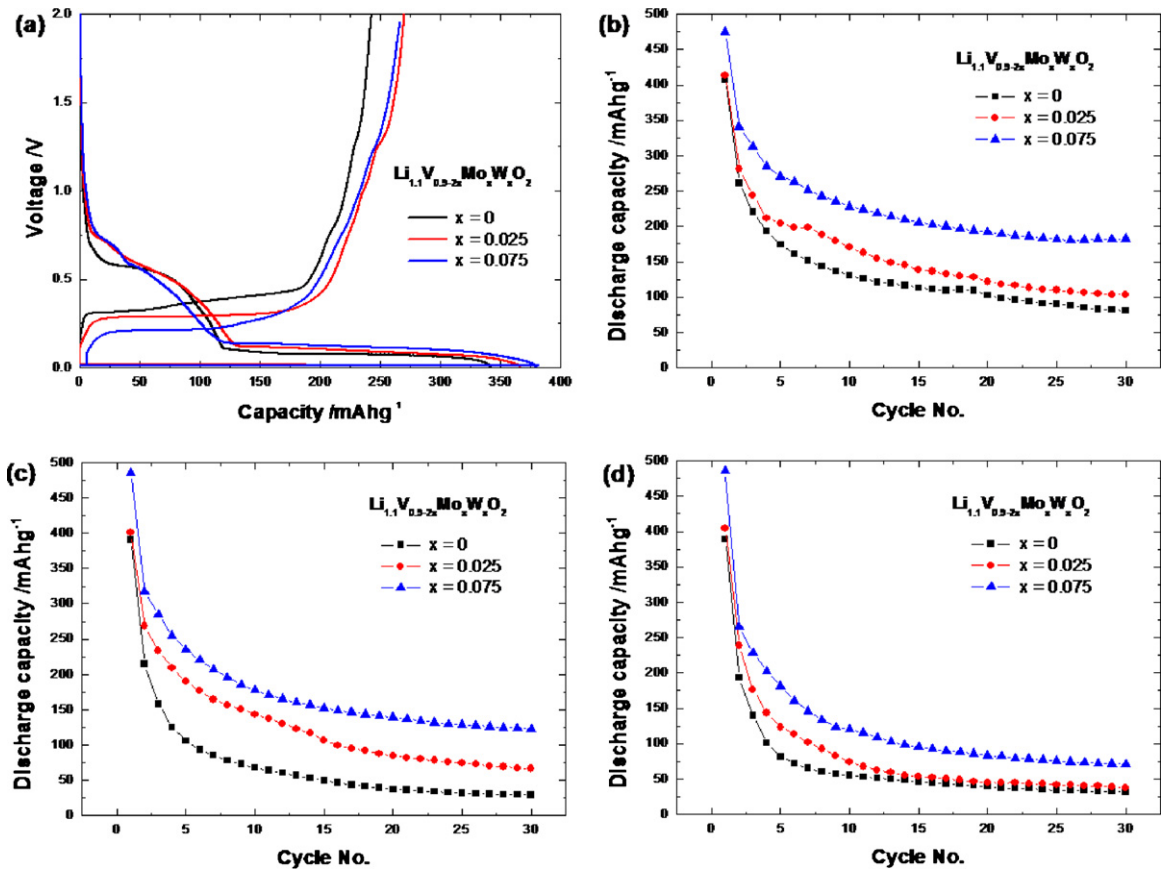

Fig. 3. Battery performances of $Li_{1.1}V_{0.9-2x}Mo_xW_xO_2$ ($x = 0$, 0.025, 0.075) anodes: (a) voltage profile at 0.1 C, and capacity versus cycle number at (b) 0.1 C, (c) 1 C, and (d) 5 C.

Table 1
Occupied states of $Li_{1.1}V_{0.9}O_2$ and $Li_{1.1}V_{0.8}Mo_{0.05}W_{0.05}O_2$.

Sample	Atom	s	p	d	F	Charge
$Li_{1.1}V_{0.9}O_2$ $E_F = -8.889$ eV	Li	2.206	0.443	0.098	0	+0.254
	V	0.403	6.661	3.615	0	+0.301
	O	1.809	4.467	0	0	−0.272
$Li_{1.1}V_{0.8}Mo_{0.05}W_{0.05}O_2$ $E_F = -8.834$ eV	Li	2.202	0.441	0.098	0	+0.258
	V	0.404	6.662	3.644	0	+0.294
	Mo	0.376	6.539	3.854	0.395	+0.846
	W	0.684	6.879	4.066	14.386	+0.003
	O	1.809	4.473	0	0	−0.278

in the charge difference after doping. However, as seen in Table 1, the electronic charge clearly increases upon doping for Li (from +0.254 to +0.258) and for O (from −0.272 to −0.278). Such an increase in charge difference could increase the Coulombic interactions between the Li and O layers, and thus decrease the lattice parameter for the *c*-axis. Therefore, even though the bond lengths between V and O increase, the *c*-axis lattice parameter is decreased because of the much greater effect of the increased Coulombic interactions between the Li and O layers.

In general, the decrease in the lattice parameter on the *c*-axis in the layered structure could lead to a decrease in the Li diffusion coefficient because of the more difficult insertion or extraction. However, the galvanostatic charge/discharge test showed quite the opposite result. As shown in Fig. 3, the discharge capacity was increased by about 55% for 0.1 C, and by 140% for 1 C, and 135% for 5 C at 5 cycles, which implies that the capacity increase is much more marked at high *C*-rates. Such increases in rate capability seem to be contradictory to the *c*-axis contraction after doping. The main origin of this marked rate-capability enhancement is therefore attributed to the increase in electronic conductivity due to the extra free electron donated mainly by Mo after doping, as clearly identified from the first-principle calculations. The enhanced electronic conductivity also lowers the potential loss due to the IR drop, so that an increase in the doping level results in an increase in charge potential and a decrease in discharge potential, which are advantageous properties for anode materials.

4. Conclusions

$Li_{1.1}V_{0.9-2x}Mo_xW_xO_2$ powders were synthesized by a solid-state reaction. On the basis of the calculation of their electronic structure using the FEFF 8.4 code, the origin of the enhanced cell performance upon doping was investigated from the viewpoint of the lattice structure and change in electron density. The doping gave rise to changes in lattice parameters and electron density through the generation of an extra free electron. The effect of W on the lattice parameter and the carrier density was marginal in comparison

with Mo, because its d-band structure was too broad to exhibit effective interactions with the V 3d and O 2p bands. Therefore, the increased electronic conductivity due to the extra free electron is the main origin of the enhanced charge/discharge capacity and rate capability.

Acknowledgements

This work was funded by "The Middle and Long-term Technology Development Project" of the Ministry of Knowledge Economy of Korea, the National Research Foundation of Korea Grant funded by the Korean Government(MEST) (2012-0000172, 2011-0027954), and a creativity program by the Korea Institute of Science and Technology, Republic of Korea.

References

[1] S. Denis, E. Baudrin, F. Orsini, G. Ouvrard, M. Touboul, J.-M. Tarascon, J. Power Sources 81–82 (1999) 79.
[2] S. Kim, H. Ikuta, M. Wakihara, Solid State Ionics 139 (2001) 57.
[3] T. Morishita, K. Nomura, T. Inamasu, M. Inagaki, Solid State Ionics 176 (2005) 2235.
[4] N. Choi, J. Kim, R. Yin, S. Kim, Mater. Chem. Phys. 116 (2009) 603.
[5] H. Kim, B. Cho, Bull. Korean Chem. Soc. 31 (2010) 1267.
[6] J. Song, H. Park, K. Kim, Y. Jo, J. Kim, Y. Jeong, Y. Kim, J. Power Sources 195 (2010) 6157.
[7] R. Yin, Y. Kim, W. Choi, S. Kim, H. Kim, Adv. Quantum Chem. 54 (2008) 23.
[8] J. Goodenough, G. Dutta, A. Manthiram, Phys. Rev. B 43 (1991) 10170.
[9] S. Lee, H. Kim, T. Seong, J. Alloys Compd. 509 (2011) 3136.
[10] A.L. Ankudinov, B. Ravel, J.J. Rehr, S.D. Conradson, Phys. Rev. B 58 (1998) 7565.